

Supporting Information

Kapishnikov et al. 10.1073/pnas.1118134109

SI Text

SI Materials and Methods. Note on Fe fluorescence vs. hemozoin crystal thickness. The purpose of this note is to show how one can transform the Fe fluorescence map of a red blood cell to a thickness map of the hemozoin (hz) crystals. An example of a Fe fluorescence map is shown in Fig. S4.

The basic idea in converting this map to a thickness map is to compare the intensity levels to those from a known Fe sample. For this we used a Fe foil of thickness 25.67 micron inserted into exactly the same X-ray beam.

With a planar Fe foil, as shown in Fig. S5, having its normal tilted at an angle β relative to the beam and with the fluorescent detector axis at an angle α from 90° , one can evaluate the ratio of fluorescent intensity to that of the direct beam (see equation 7.22, p. 255, ref. 1):

$$I_f/I_0 = \varepsilon \cdot (\Delta\Omega/4\pi) e^{-a\mu_f d'} \frac{\mu}{\mu - a\mu_f} \{1 - e^{-(\mu - a\mu_f)d'}\}, \quad [\text{S1}]$$

where $a = \cos\beta / \sin(\alpha + \beta)$ and d' is the foil thickness divided by $\cos\beta$. The solid angle subtended by the detector is $\Delta\Omega$ and ε is the probability that an absorption process results in X-ray fluorescence and not in an Auger electron. The inverse absorption lengths at the incident energy and at the fluorescent energy are denoted as μ and μ_f , respectively.

Note that as the thickness of the foil tends to zero the expression simplifies to

$$I_f/I_0 \rightarrow \varepsilon \cdot (\Delta\Omega/4\pi) \mu d'. \quad [\text{S2}]$$

A “foil” of hemozoin has much less density of Fe atoms than an iron foil, so in that case we can use Eq. S2 with $d' = (\rho_{\text{hemozoin}}/\rho_{\text{Fe}})d_{\text{hemozoin}}$. We can therefore relate the observed fluorescent intensity from RBC to that from the Fe foil by the following formula:

$$I_{\text{Fe}}/I_{\text{hemozoin}} = \frac{e^{-a\mu_f d'} \frac{\mu}{\mu - a\mu_f} \{1 - e^{-(\mu - a\mu_f)d'}\}}{(\rho_{\text{hemozoin}}/\rho_{\text{Fe}})\mu d_{\text{hemozoin}}} \quad [\text{S3}]$$

$$\mu d_{\text{hemozoin}} = \frac{I_{\text{hemozoin}} [\text{cts/sec}]}{I_{\text{Fe}} [\text{cts/sec}] \rho_{\text{hemozoin}}} \frac{\rho_{\text{Fe}}}{\rho_{\text{hemozoin}}} e^{-a\mu_f d'} \frac{\mu}{\mu - a\mu_f} \{1 - e^{-(\mu - a\mu_f)d'}\}.$$

In our actual experiment, the X-ray energy was 9 keV, giving an inverse absorption length of $\mu = 0.178 \text{ micron}^{-1}$. The inverse absorption length at the fluorescent energy 6.4 keV is $\mu_f = 0.0539 \text{ micron}^{-1}$. The angles were $\alpha = 14^\circ$ and $\beta = 20^\circ$, giving $a = 1.68$ and $d' = 27.32 \text{ micron}$. The fluorescent intensity from the foil was 150,400 cts/sec. The ratio of Fe density in the foil and in hemozoin crystals is 59.5, because the bcc unit cell of Fe has a volume of 2.87^3 \AA^3 , whereas a unit cell of hemozoin has a volume of $1,407 \text{ \AA}^3$. In both cases there are two Fe atoms per unit cell, so the density ratio is simply the unit cell volume ratio $1,407/2.87^3 = 59.5$. With these numbers inserted into Eq. S3 we then find $d_{\text{hemozoin}}[\mu] = 3.46 \cdot 10^{-4} \cdot I_{\text{hemozoin}}[\text{cts/sec}]$. From Fig. 1 we have a typical Fe fluorescence

of 50 cts per 0.2 s, or 250 cts/sec, corresponding to a hemozoin thickness in that pixel of $0.087 \text{ \mu m} = 87 \text{ nm}$.

Probability of observing one or more (hkl) Bragg reflections. A one-dimensional crystal with unit cells at positions $n \cdot a$, $n = 1 \dots N$, diffracting the incident wave vector k to k' thus implying the wavevector $Q = k - k'$, will provide a scattered amplitude $A(Q) = \sum_{n=1}^N e^{iQ(na)}$. Assume tacitly that Q is parallel to the crystal and has a relative deviation, ζ , from the Bragg point—i.e., $Q = (2\pi/a)[1 + \zeta]$. It follows that the magnitude of the amplitude is $|A(\zeta)| = \sin(\pi N\zeta)/(\pi\zeta)$. The intensity, proportional to $|A(Q)|^2$, has FWHM $0.88/N$, peak height N^2 , and area N . This result is depicted in the Fig. S6 (Upper Right)—i.e., $\Delta G/G \approx 1/N$ or more precisely $[\Delta G/G]_{\text{FWHM}} = 0.88/N$.

The Debye–Scherrer cone. Bragg scattering from a crystalline powder is depicted in Fig. S6 (Lower Left). The direction of reciprocal lattice vectors, which are denoted G , from the crystallites will normally be randomly distributed on the sphere with radius $|G|$. The Laue condition for Bragg reflection is $k - k' \equiv Q = G$, so $2k \sin\theta = G$. The incident wavevector k is the vertical black line terminating in the origin for the sphere, and k' must be somewhere on the cone with an apex opening angle of $2 \cdot 2\theta$ —the so-called Debye–Scherrer cone. Two possibilities for the termination of k' are shown as the points A and B—they are special because they lie in two great circle planes that are perpendicular to each other. In the projection view (Lower Right), point B is in the drawing plane and point A is perpendicular above the drawing plane.

The sphere of terminating reciprocal lattice points is not an infinitely thin sphere, because of the finite size of a crystallite. The finite number of Bragg planes, both along G and in the two transverse directions, implies a smearing, ΔG , of G , so the Bragg “point” actually becomes a Bragg “cube” with cube length ΔG . Consequently, the Debye–Scherrer ring acquires a finite height $H = \Delta G \cos\theta$. As seen from the projection view, the radius of the Debye–Scherrer ring is $R = k \sin 2\theta = [G/(2 \sin\theta)] \sin 2\theta = G \cos\theta$, and the area is $H \cdot 2\pi R$. The probability that a crystallite will Bragg reflect is this area relative to the area of the upper half-sphere [half-sphere because (h, k, l) and $(\bar{h}, \bar{k}, \bar{l})$ reflections are degenerate]—i.e., the probability for observing the (h, k, l) Bragg reflection from one crystallite is $2\pi R \cdot H/(2\pi R^2) = H/R = \Delta G \cos\theta/G \cos\theta = \Delta G/G \approx 1/N$. We can now estimate the probability for observing several Bragg reflections with the same (h, k, l) .

The unit cell size of hz is of order 10 \AA or 1 nanometer. A typical number of Bragg planes for reflection is therefore the crystal size, say 100 nanometers relative to 1 nanometer (i.e., $N = 100$). Suppose the powder is just the number of hz crystals in an infected red blood cell (i.e., of order of 10). The probability for observing say one (h, k, l) reflection is $p_1 = \text{number of crystallites}/N \approx 0.1$. The probability of observing n Bragg reflections would be p_1^n if the hz crystallites were randomly oriented. Our data set is in fairly good accordance with this estimate for $n = 1$, but not at all in accordance for $n \geq 2$, so the inevitable conclusion is that the orientation of the individual hemozoin crystals are not at all random.

1. Als-Nielsen J, McMorrow D (2011) *Elements of Modern X-ray Physics* (Wiley, New York), 2nd Ed.

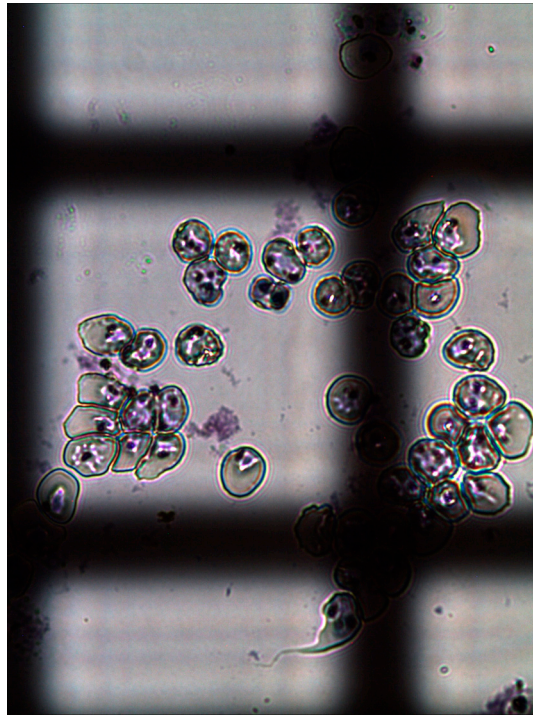


Fig. S1. Optical micrograph of *Plasmodium*-infected RBCs stained in Giemsa solution, smeared onto a 50- μ thick, 10-mm diameter glass plate. Note the grid of labeled Cu bars with a square size of 63 μ m glued on the opposite side of the smear.

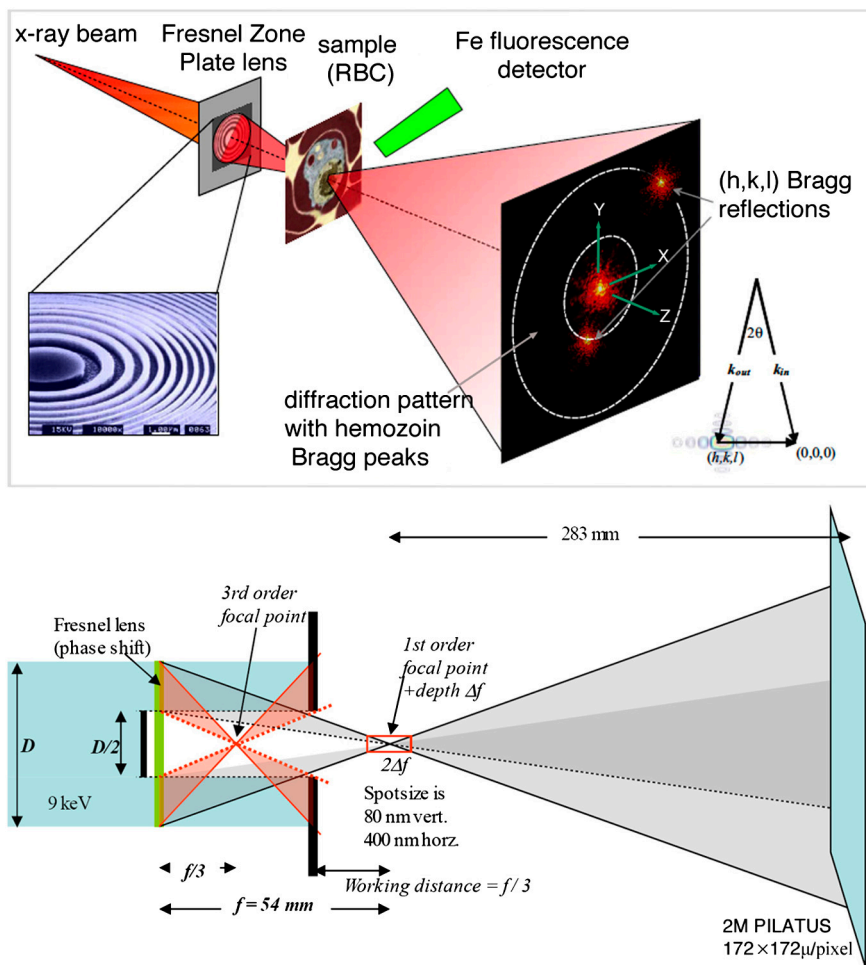


Fig. S2. The nanofocus X-ray beam experimental setup at the cSAXS beamline of the Swiss Light Source. (*Top*) A schematic view of the experimental setup. A submicron-diameter monochromatic X-ray beam was obtained by a phase-inverting Fresnel lens. A central beam stop and an order-sorting aperture focused the incident beam diameter of $150\ \mu\text{m}$ down to a focal spot of $400\ \text{nm}$ in the horizontal and $80\ \text{nm}$ in the vertical direction. The Fe fluorescence signal has been collected onto an energy dispersive fluorescent detector situated in the horizontal plane, 76° from the beam direction. The X-ray diffraction signal has been collected onto the 2-megapixel PILATUS area detector situated $283\ \text{mm}$ downstream from the sample. The scan is performed by moving the sample holder in steps of not more than $400\ \text{nm}$ in lateral and $80\ \text{nm}$ in transverse directions. Based on knowledge that density of Fe atoms in hemozoin is much higher than in hemoglobin and anywhere else in the sample, the step duration has been adjusted to be shorter (typically, $0.1\ \text{s}$) while the Fe fluorescence X-ray signal is lower than an empirically derived threshold value (short scan) and longer when the accumulated signal is higher than the threshold (long scan). During the long scans the diffraction signal has been registered onto the PILATUS detector. The long scan acquisition time was $0.25\ \text{s}$ plus time needed for storing the 2D signal data acquired on the PILATUS detector (about $0.75\ \text{s}$). This scanning scheme has been based upon assumption that there is no hemozoin material at the low Fe fluorescence signal intensities, and therefore there is no diffraction signal to collect. (*Bottom*) A detailed view of the X-ray focusing setup.

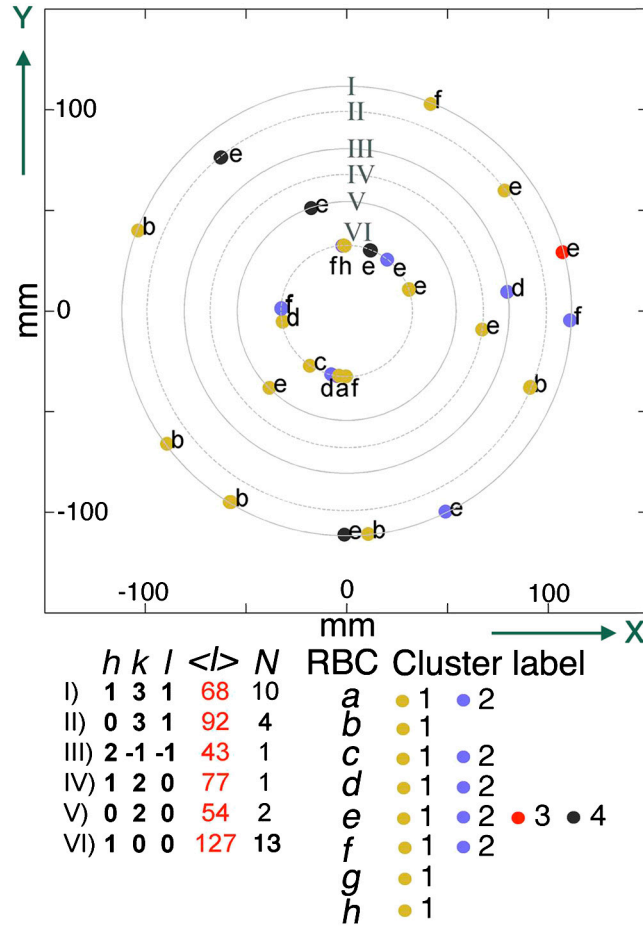


Fig. S3. X-ray diffraction patterns on the PILATUS detector from the different hemozoin color-labeled clusters in the RBCs of sample 1. A list is given of the different (h, k, l) X-ray reflections observed, their averaged intensities $\langle I(h, k, l) \rangle$, and number observed. The detector axes are labeled here and in Fig. 2 and Fig. S2.

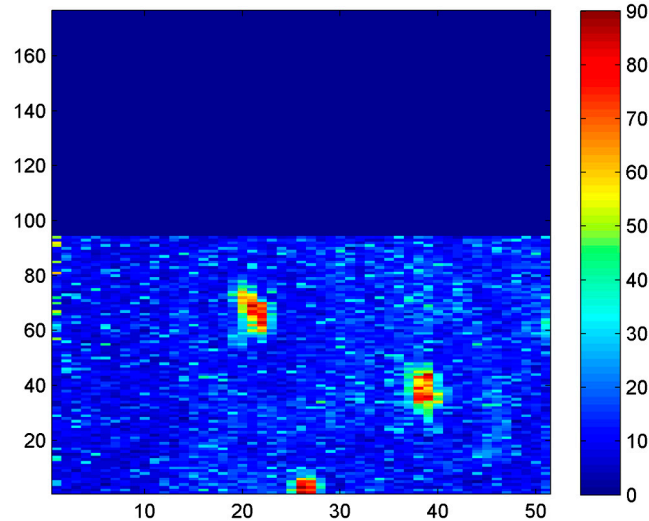


Fig. S4. The figure shows the Fe fluorescence yield vs. the hitting point of the X-ray beam, which has dimensions 400 nm along the horizontal axis and 80 nm along the vertical axis, corresponding to the pixels in the plot. The upper part with zero intensity was not irradiated, so it is only the lower half that is of interest to us. The exposure time was 0.25 s per pixel.

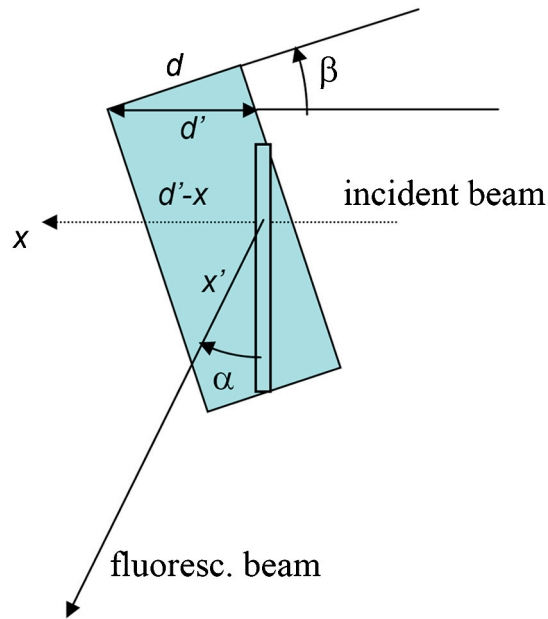


Fig. S5. The incident beam is at angle β relative to the foil normal, and the fluorescence detector is at angle $\pi/2 - \alpha$ relative to the foil normal. The foil is much wider than shown in the figure. One considers an absorption process taking place in a thin slab after the X-ray photon has penetrated a thickness x into the foil. The fluorescent X-ray photon has to traverse a distance x' in the foil.

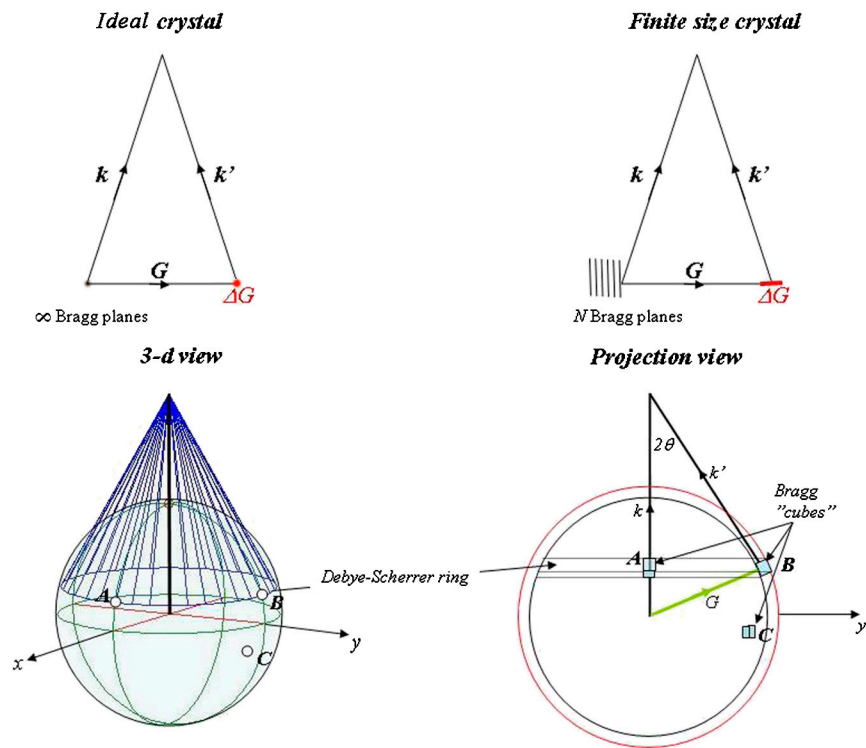


Fig. S6. Diffraction geometry.